

KA-TP-22-1999

November 1999

Possible enhancement of the $e^+e^- \rightarrow H^\pm W^\mp$ cross section in the two-Higgs-doublet model

Shinya Kanemura ¹

*Institut für Theoretische Physik der Universität Karlsruhe
D-76128 Karlsruhe, Germany*

Abstract

The production process of the charged Higgs-boson associated with a W boson is discussed at electron-positron colliders in the general two-Higgs-doublet model (2HDM) as well as the minimal supersymmetric standard model (MSSM). This process is induced at one-loop level in these models. We investigate possible enhancement of the cross section due to the quark and Higgs one-loop effects under available experimental constraints and requirement from validity of perturbation theory. In the MSSM, quadratic mass effects of the top quark enlarge the cross section, while the Higgs-loop effects are very small because of the decoupling theorem. In the non-SUSY 2HDM, in addition to the large top-quark mass effects for small $\tan\beta$ region, the cross section can be enhanced by the Higgs non-decoupling effects in the intermediate $\tan\beta$ region. These effects are rapidly reduced for larger $\tan\beta$ region by the constraint from validity of perturbation theory.

PACS: 12.60.Fr; 14.80.Cp

Keywords: Charged Higgs Bosons, Two Higgs Doublet Models

¹e-mail: kanemu@particle.physik.uni-karlsruhe.de

1 Introduction

The Higgs sector has not yet been confirmed experimentally. In near future, a neutral Higgs boson may be discovered at Tevatron II or LHC, by which the standard picture of particle physics is completed. The exploration of additional Higgs bosons will be then very important to confirm extended Higgs sectors. Actually various theoretical insights suggest such extensions from the minimal Higgs sector with one Higgs doublet; the supersymmetry (SUSY), extra CP-violating phases, a source of neutrino masses, the strong CP problem and so on. Most of the extended Higgs models include charged Higgs bosons. Discovery of a charged Higgs boson, H^\pm , directly shows these extended versions of the Higgs sector. At LHC, search of these extra Higgs bosons is also one of the most important tasks. In addition, considerable precision measurement of high energy phenomena may be possible at future linear colliders (LC's) [1].

In this paper, we discuss the charged Higgs boson production process associated with a W boson at LC's, $e^+e^- \rightarrow H^\pm W^\mp$, in the general two-Higgs-doublet model (2HDM) including the minimal supersymmetric standard model (MSSM). Neglecting the electron mass, the tree-level contribution to this process disappears in these models because of no tree-level $H^\pm W^\mp V$ couplings ($V = \gamma$ and Z^0). Because these couplings occur at one-loop level [2, 3], the process $e^+e^- \rightarrow H^\pm W^\mp$ is one-loop-induced. At LC's, the H^\pm pair production [4] is one of the main processes for the charged Higgs search, whose cross section may be large enough to be detected if H^\pm is much lighter than $\sqrt{s}/2$. This process rapidly decreases for heavier H^\pm even if the mass is below the threshold. The process $e^+e^- \rightarrow H^\pm W^\mp$ then becomes important as a complementary process if it is enhanced enough. Our question here is how much this loop-induced process can be enhanced in the non-SUSY 2HDM as well as in the MSSM [5].

In general, in the MSSM, one-loop effects of heavy super-particles including extra Higgs bosons are small because of the decoupling theorem [6], so that only the quark mass effects contribute to the large one-loop effects. In our process, the enhancement due

to quark mass effects occurs for small $\tan\beta$ region, because the $\tan\beta$ dependence of the quark mass effects is $\sim m_t^2 \cot\beta$ ($\sim m_b^2 \tan\beta$) for large $\cot\beta$ ($\tan\beta$) in the amplitude. From the requirement of the unification at the GUT scale, the allowed region of $\tan\beta$ is $1 - 2 \lesssim \tan\beta$ in the MSSM [7]. The recent experimental results at LEP II exclude $\tan\beta$ smaller than ~ 2 [8]. Thus it may be difficult to expect a large enhancement in this case. On the other hand, in the non-SUSY 2HDM larger enhancement due to the top-quark mass is expected because smaller $\tan\beta$ is allowed than in the MSSM, which is finally bounded by the requirement of validity of perturbation theory for the top-Yukawa coupling constant [9]. In addition, the non-decoupling mass effects of the heavy Higgs bosons are also possible in this model [10]. The non-decoupling property of the Higgs sector appears if the soft-breaking mass with respect to the discrete symmetry is small [11, 12]. The cross section may be then enhanced not only by the top-quark mass effects but also by the Higgs non-decoupling mass effects in the non-SUSY 2HDM. Therefore, it is an interesting problem to examine possible enhancement of the cross section due to the effects of quarks as well as Higgs bosons under constraints from available experimental data and the perturbative unitarity [13]. Here we take account of the constraint on the ρ parameter from the data [14] and of the $b \rightarrow s\gamma$ result [15, 16].

We find that, in the MSSM, the cross section is enhanced maximally at the lower bound of $\tan\beta$ ($\sim 1 - 2$) by the top-quark mass effects, which amounts to a few 0.1 fb for 200 GeV of the H^\pm mass. The cross section rapidly decreases for larger $\tan\beta$. Our result for the MSSM is somewhat different from that in Ref [5]. In the non-SUSY 2HDM, the top-quark effects significantly enhances the cross section around the lower bound of $\tan\beta$ ($\sim 0.2 - 0.3$), where the top-Yukawa coupling becomes large closed to break validity of perturbation theory. In addition, the Higgs non-decoupling effects can contribute to the enhancement for $\tan\beta > 1$ in this case, because the Higgs effects can grow proportional to $\sim \tan\beta$ in the amplitude. For large $\tan\beta$ region ($10 \lesssim \tan\beta$), however, such Higgs effects turn out to be strongly constrained by the perturbative unitarity for the Higgs

self-coupling constants. Thus the Higgs non-decoupling effects enhance the cross section only in the intermediate regime of $\tan\beta$. For example, for the charged Higgs boson with the mass of 200 GeV in the Model II 2HDM, the cross section can become 10 (0.3) fb for $\tan\beta \sim 0.2$ (1) at $\sqrt{s} = 500$ GeV by the top-quark mass effects, while it also amounts to about 0.1 fb at $\tan\beta \sim 5 - 10$ by the non-decoupling Higgs mass effects. For larger $\tan\beta$ regime, such enhancement is strongly bounded and the cross section reduces to be invisible.

In Sec 2, the 2HDM is reviewed briefly. The calculation of the cross section is explained in Sec 3. After some analytic discussion on mass effects on the amplitude in Sec 4, we present our numerical results in Sec 5. Conclusion is given in Sec 6. In Appendix A, the relevant formulas for the MSSM Higgs sector are given. Details of the analytic results of the calculation are shown in Appendix B.

2 The model

The 2HDM with a softly-broken discrete symmetry under $\Phi_1 \rightarrow \Phi_1$, $\Phi_2 \rightarrow -\Phi_2$ is assumed here. There are then two kinds of the Yukawa sector under the this symmetry, what we call, Model I and Model II [17]. The Higgs sector is given for both Model I and II by [2]

$$\begin{aligned} \mathcal{L}_{\text{THDM}}^{\text{int}} = & \mu_1^2 |\Phi_1|^2 + \mu_2^2 |\Phi_2|^2 + \left\{ \mu_3^2 (\Phi_1^\dagger \Phi_2) + \text{h.c.} \right\} \\ & - \lambda_1 |\Phi_1|^4 - \lambda_2 |\Phi_2|^4 - \lambda_3 |\Phi_1|^2 |\Phi_2|^2 - \lambda_4 \left(\text{Re} \Phi_1^\dagger \Phi_2 \right)^2 - \lambda_5 \left(\text{Im} \Phi_1^\dagger \Phi_2 \right)^2. \end{aligned} \quad (1)$$

This potential includes the MSSM Higgs sector as a special case. By neglecting CP-violating phases, we have five massive eigenstates from the doublets Φ_1 and Φ_2 ($\langle \Phi_i \rangle \equiv v_i/\sqrt{2}$ and $\sqrt{v_1^2 + v_2^2} = 246$ GeV); that is, two CP-even neutral bosons (h^0 and H^0 , diagonalized by the mixing angle α ; we define that h^0 is lighter than H^0 .), one pair of the charged Higgs boson H^\pm , and one CP-odd neutral A^0 Higgs boson, as well as three Nambu-Goldstone bosons (w^\pm and z^0). In addition to the four mass parameters m_{h^0} , m_{H^0} , m_{H^\pm}

and m_{A^0} , we have two mixing angles α and β ($\tan \beta = v_2/v_1$) and one free dimension-full parameter M corresponding to the soft-breaking mass ($M^2 \equiv \mu_3^2/(\sin \beta \cos \beta)$). Relations among the coupling constants and the masses are given then by

$$\lambda_1 = \frac{1}{2v^2 \cos^2 \beta} (\cos^2 \alpha m_{H^0}^2 + \sin^2 \alpha m_{h^0}^2 - \sin^2 \beta M^2), \quad (2)$$

$$\lambda_2 = \frac{1}{2v^2 \sin^2 \beta} (\sin^2 \alpha m_{H^0}^2 + \cos^2 \alpha m_{h^0}^2 - \cos^2 \beta M^2), \quad (3)$$

$$\lambda_3 = \frac{\sin 2\alpha}{v^2 \sin 2\beta} (m_{H^0}^2 - m_{h^0}^2) + \frac{2m_{H^\pm}^2}{v^2} - \frac{1}{v^2} M^2, \quad (4)$$

$$\lambda_4 = -\frac{2m_{H^\pm}^2}{v^2} + \frac{2}{v^2} M^2, \quad (5)$$

$$\lambda_5 = \frac{2}{v^2} (m_{A^0}^2 - m_{H^\pm}^2). \quad (6)$$

The formulas for the MSSM Higgs sector are obtained from (2) - (6) by imposing the relation among the parameters, which is shown in Appendix A.

The Yukawa interaction with respect to the charged Higgs boson is expressed in Model II by

$$\mathcal{L}_{Htb} = \bar{b} \left\{ \frac{m_b}{\sqrt{2}v} \tan \beta (1 - \gamma_5) + \frac{m_t}{\sqrt{2}v} \cot \beta (1 + \gamma_5) \right\} t H^- + \text{h.c.} \quad (7)$$

The $\tan \beta$ in the m_b term is replaced by $\cot \beta$ in the case of Model I [17].

3 $e^+ e^- \rightarrow H^- W^+$

We consider the process $e^-(\tau, k) + e^+(-\tau, \bar{k}) \rightarrow H^-(p) + W^+(\bar{p}, \bar{\lambda})$, where $\tau = \pm 1$ and $\bar{\lambda} = 0, \pm 1$ are helicities of the electron and the W boson; k and \bar{k} are incoming momenta of the electron and the positron; p and \bar{p} are outgoing momenta of H^- and W^+ , respectively. The helicity amplitude may be written by

$$\mathcal{M}(k, \bar{k}, \tau; p, \bar{p}, \bar{\lambda}) = \sum_{i=1}^3 F_{i,\tau}(s, t) K_{i,\tau}(k, \bar{k}, \tau; p, \bar{p}, \bar{\lambda}), \quad (8)$$

where the form factors $F_{i,\tau}(s, t)$ include all the dynamics that depends on the model. The kinematical factors are expressed by

$$K_{i,\tau}(k, \bar{k}, \tau; p, \bar{p}, \bar{\lambda}) = j_\mu T_i^{\mu\beta} \epsilon_\beta(\bar{p}, \bar{\lambda})^*, \quad (9)$$

where j_μ is the electron current and $\epsilon_\beta(\bar{p}, \bar{\lambda})^*$ is the polarisation vector of the W boson. The basis tensors $T_i^{\mu\beta}$ are defined by

$$T_1^{\mu\beta} = g^{\mu\beta}, \quad (10)$$

$$T_2^{\mu\beta} = \frac{1}{m_W^2} P^\mu P^\beta, \quad (11)$$

$$T_3^{\mu\beta} = \frac{i}{m_W^2} \epsilon^{\mu\beta\rho\sigma} P_\rho q_\sigma, \quad (12)$$

where $P^\mu \equiv p^\mu - \bar{p}^\mu$, $q^\mu \equiv p^\mu + \bar{p}^\mu = k^\mu + \bar{k}^\mu$ and $\epsilon^{0123} = -1$. We list the explicit expression of each $K_{i,\tau}$ in the center-of-mass frame in Table 1 by using β_{HW} and the scattering angle Θ defined by

$$\beta_{HW} = \sqrt{1 - \frac{2(m_W^2 + m_{H^\pm}^2)}{s} + \frac{(m_W^2 - m_{H^\pm}^2)^2}{s^2}}, \quad (13)$$

$$\cos \Theta = \frac{2t + s - m_{H^\pm}^2 - m_W^2}{s\beta_{HW}}, \quad (14)$$

where s and t are the Mandelstam variables ($s = (k + \bar{k})^2 + (p + \bar{p})^2$, $t = (k + \bar{k})^2 + (p - \bar{p})^2$).

The total cross section is calculated according to the formula

$$\sigma(s) = \frac{1}{16\pi} \frac{1}{s^2} \int_{t_{\min}}^{t_{\max}} \frac{1}{2} \frac{1}{2} \sum_\tau \sum_\lambda |\mathcal{M}(k, \bar{k}, \tau; p, \bar{p}, \bar{\lambda})|^2 dt, \quad (15)$$

where t_{\max} and t_{\min} are defined by

$$t_{\max} = \frac{1}{2}(m_{H^\pm}^2 + m_W^2 - s + s\beta_{HW}), \quad (16)$$

$$t_{\min} = \frac{1}{2}(m_{H^\pm}^2 + m_W^2 - s - s\beta_{HW}). \quad (17)$$

In calculation, the form factors $F_{i,\tau}(s, t)$ may be decomposed according to the type of Feynman diagrams (Fig 1) as

$$F_{i,\tau}(s, t) = F_{i,\tau}^\gamma(s) + F_{i,\tau}^Z(s) + F_{i,\tau}^t(s, t) + F_{i,\tau}^{Box}(s, t), \quad (18)$$

where $F_{i,\tau}^V$ ($V = \gamma$ and Z) are the contribution from the one-loop induced H^-W^+V vertices (Fig 1(a)). The $H^+W_\mu^-V_\nu^0$ vertices are defined as $igm_W V_{\mu\nu}^{HWV}$ (Fig 2), in which $V_{\mu\nu}$ may be expressed by [2, 3]

$$\begin{aligned} V_{\mu\nu}^{HWV}(p_H, p_W, p_V) &= F^{HWV}(p_H, p_W, p_V)g_{\mu\nu} + G^{HWV}(p_H, p_W, p_V)\frac{p_{V\mu}p_{W\nu}}{m_W^2} \\ &\quad + iH^{HWV}(p_H, p_W, p_V)\frac{p_V^\rho p_W^\sigma}{m_W^2}\epsilon_{\mu\nu\rho\sigma}, \end{aligned} \quad (19)$$

where p_H is the incoming momentum of H^- , and p_V ($V = Z$ or γ) and p_W are outgoing momenta of V and W bosons, respectively. The form factor $F_{i,\tau}^V(s)$ are then expressed by

$$F_{1,\tau}^V(s) = gm_W C_V \frac{1}{s - m_V^2} F^{HWV}(m_W^2, s, m_{H^\pm}^2), \quad (20)$$

$$F_{2,\tau}^V(s) = gm_W C_V \frac{1}{s - m_V^2} \frac{1}{2} G^{HWV}(m_W^2, s, m_{H^\pm}^2), \quad (21)$$

$$F_{3,\tau}^V(s) = gm_W C_V \frac{1}{s - m_V^2} \frac{-1}{2} H^{HWV}(m_W^2, s, m_{H^\pm}^2), \quad (22)$$

where m_V is mass of the neutral gauge bosons (m_Z and $m_\gamma (= 0)$), and C_V are defined by $C_\gamma = eQ_e$ and $C_Z = g_Z(T_e^3 - s_W^2 Q_e)$ ($e = gs_W = g_Z s_W c_W$), in which $Q_e = -1$, and $T_e^3 = -1/2$ (0) for the electron with the helicity $\tau = -1$ (+1). The explicit formulas of the F^{HWV} , G^{HWV} , H^{HWV} are given in Appendix B. 1. The $F_{i,\tau}^t(s, t)$ is of the t channel diagram with the one-loop H^-W^+ mixing diagrams (Fig 1(b)) and the box diagram contributions are expressed by $F_{i,\tau}^{Box}$ (Fig 1(c)). We also show the explicit results for $F_{i,\tau}^t$ and $F_{i,\tau}^{Box}$ in Appendix B. 2 and B. 3, respectively.

4 Non-decoupling mass effects

Let us consider the case in which the one-loop amplitude is largely enhanced. At first, as for the quark mass effect, the contribution to the amplitude is proportional to $\sim m_t^2 \cot \beta - m_b^2 \tan \beta$ in Model II, because one tbH^\pm Yukawa coupling (7) is included in each quark-loop diagram. Thus we expect that the amplitude is enhanced for small $\tan \beta$ region ($\tan \beta < 1$) because of $m_t \gg m_b$. Since the $\tan \beta$ dependence of the amplitude is linear, not quadratic,

the bottom quark mass effect should be small even for large $\tan\beta$. In Model I, $\tan\beta$ is just replaced by $\cot\beta$ in the coefficient above. Thus in both Model I and II, we expect that enhancement of the cross section due to the top-quark effects occurs for small $\tan\beta$ region.

Next, we discuss the Higgs mass effects. The non-decoupling effects of the Higgs boson masses appear only when the Higgs sector has a special property, on which all the Higgs mass squared are expressed like $\sim \lambda_i v^2$, where λ_i is some combination of the Higgs self-coupling constants. In this case, the decoupling theorem [6] does not work and we expect that the effects of $\mathcal{O}(m_H^2/v^2)$ appears similar to the case of the quark effects. In general, the mass squared of the heavier Higgs bosons takes the form proportional to $\sim \mathcal{O}(\lambda_i v^2) + M^2$, where M represents the soft-breaking mass. In the case of $M^2 \gg \lambda_i v^2$, the masses are controlled by M and are approximately independent of λ_i , so that the effects of the heavy Higgs bosons decouple in the large mass limit [11]. The MSSM Higgs sector corresponds to this case, where λ_i are fixed to be the same order of gauge coupling constants g^2 and thus large masses of the heavier Higgs bosons are possible only by taking the large soft-breaking mass. Thus there is no large Higgs effects in the MSSM. On the other hand, in the non-SUSY 2HDM with the small soft-breaking mass M , the mass effects of heavy Higgs bosons may contribute to the enhancement of the amplitude in addition to the quark mass effects.

In order to see the non-decoupling effects analytically, let us consider one limiting case. The quadratic mass contribution is extracted from the full expression of the amplitude by taking the case of $m_W, m_{H^\pm} \ll \sqrt{s} \ll m_X$, where $m_X = m_t, m_{h^0}, m_{H^0}$ and m_{A^0} ;

$$\begin{aligned}
& \mathcal{M}(k, \bar{k}, \tau; p, \bar{p}, \bar{\lambda} = 0) \\
&= \sin\Theta \frac{g^2}{c_W^2} \frac{T_e^3}{16\pi^2 v^2} \left[\frac{3}{2} \left\{ \frac{m_{H^0}^2 m_{A^0}^2}{m_{H^0}^2 - m_{A^0}^2} \ln \frac{m_{H^0}^2}{m_{A^0}^2} - \frac{m_{h^0}^2 m_{A^0}^2}{m_{h^0}^2 - m_{A^0}^2} \ln \frac{m_{h^0}^2}{m_{A^0}^2} \right\} J(\alpha, \beta) \right. \\
&\quad - \left\{ \frac{c_{2W}}{2} m_{H^0}^2 + \frac{3}{4} \frac{m_{H^0}^2 m_{A^0}^2}{m_{H^0}^2 - m_{A^0}^2} \ln \frac{m_{H^0}^2}{m_{A^0}^2} \right\} K(\alpha, \beta) \\
&\quad \left. - \left\{ \frac{c_{2W}}{2} m_{h^0}^2 + \frac{3}{4} \frac{m_{h^0}^2 m_{A^0}^2}{m_{h^0}^2 - m_{A^0}^2} \ln \frac{m_{h^0}^2}{m_{A^0}^2} \right\} L(\alpha, \beta) - \frac{N_c}{2} m_t^2 \cot\beta \right]
\end{aligned}$$

$$\begin{aligned}
& + \sin \Theta \frac{g^2 s_W^2 Q_e}{16\pi^2 v^2} \left[\frac{3}{2} \left\{ \frac{m_{H^0}^2 m_{A^0}^2}{m_{H^0}^2 - m_{A^0}^2} \ln \frac{m_{H^0}^2}{m_{A^0}^2} - \frac{m_{h^0}^2 m_{A^0}^2}{m_{h^0}^2 - m_{A^0}^2} \ln \frac{m_{h^0}^2}{m_{A^0}^2} \right\} J(\alpha, \beta) \right. \\
& - \left\{ \frac{1}{2c_W^2} m_{H^0}^2 - \frac{3}{4} \frac{m_{H^0}^2 m_{A^0}^2}{m_{H^0}^2 - m_{A^0}^2} \ln \frac{m_{H^0}^2}{m_{A^0}^2} \right\} K(\alpha, \beta) \\
& \left. - \left\{ \frac{1}{2c_W^2} m_{h^0}^2 - \frac{3}{4} \frac{m_{h^0}^2 m_{A^0}^2}{m_{h^0}^2 - m_{A^0}^2} \ln \frac{m_{h^0}^2}{m_{A^0}^2} \right\} L(\alpha, \beta) + \frac{N_c}{2c_W^2} m_t^2 \cot \beta \right] + \mathcal{O} \left(\frac{s}{m_X^2} \right), \quad (23)
\end{aligned}$$

where

$$J(\alpha, \beta) = \sin(\alpha - \beta) \cos(\alpha - \beta), \quad (24)$$

$$K(\alpha, \beta) = \sin^2 \alpha \cot \beta - \cos^2 \alpha \tan \beta, \quad (25)$$

$$L(\alpha, \beta) = \cos^2 \alpha \cot \beta - \sin^2 \alpha \tan \beta. \quad (26)$$

From the expression (23), we expect that the amplitude is enhanced by the quadratic mass effects of the top-quark as well as the heavier Higgs bosons. The Higgs mass effects can be enhanced for the large and small $\tan \beta$ regime by the coefficients $K(\alpha, \beta)$ and $L(\alpha, \beta)$, respectively (See (24) - (26)).

The 2HDM with the non-decoupling property ($M \sim 0$) receives rather strong theoretical and experimental constraints. First, too large quadratic mass effects clearly break the validity of perturbation. There are upper bounds for the Higgs boson masses (not only of the lightest but also of all the others) [13]. In order to have the constraint as a combination among masses, mixing angles and the soft-breaking mass, we here assume that all the self-coupling constants should not be large; we set a rather conservative criterion;

$$|\lambda_i| < 8\pi, \quad (27)$$

where λ_i , ($i = 1, \dots, 5$) is the Higgs self-coupling constants defined in eqs. (2) - (6). Then, for example, from (2), we have

$$(m_{H^0}^2 - M^2) \tan^2 \beta < 16\pi v^2, \quad (28)$$

for the case of $\alpha = \beta - \pi/2$. This means that it is difficult to take large m_{H^0} and large $\tan \beta$ simultaneously with $M^2 \sim 0$. Second, the 2HDM is constrained from the precision

experimental data [14], especially the ρ parameter. The extra contribution of the Higgs sector should satisfy $\Delta\rho_{2\text{HDM}} = -0.0020 - 0.00049\frac{m_t-175\text{GeV}}{5\text{GeV}} \pm 0.0027$ [11]. In order to satisfy this condition, there are mainly two possibilities for the parameter choice; A) $m_{H^\pm}^2 \sim m_{A^0}^2$, or B) $m_{H^\pm}^2 \sim m_{H^0}^2$ ($m_{H^\pm}^2 \sim m_{h^0}^2$) with $\alpha \sim \beta - \pi/2$ ($\alpha \sim \beta$). Recent study for the $b \rightarrow s\gamma$ result [15] indicates rather conservative constraint on the charged Higgs boson mass ($m_{H^\pm} \gtrsim 165$ GeV) [16].

Taking account of all the theoretical and experimental constraints above, we realize that the best choice for the maximal enhancement by the Higgs mass effects is to take the case B) and then to choose m_{A^0} and $\tan\beta$ as much as possible within the tree unitarity constraints (27).

5 Numerical Estimation

According to the analytic discussion above, we here evaluate the cross section numerically. We fix the basic SM parameters as $\alpha_{em} = 1/128$, $s_W^2 = 0.2315$ and $M_Z = 91.19$ GeV. The top-quark mass and the bottom-quark mass are assumed to be $m_t = 175$ GeV and $m_b = 4.5$ GeV. In the MSSM, there are two free parameters in the Higgs sector, m_{H^\pm} and $\tan\beta$, and all the other parameters are related to these two by Eqs (35) - (38) in Appendix A. In the non-SUSY 2HDM, the 7 free parameters in the Higgs sector are set in the following way in order to obtain the best enhancement. As we defined the masses as $m_{h^0} < m_{H^0}$, it is better to set $\alpha = \beta - \pi/2$ (or $\alpha = 0$) for larger enhancement for $\tan\beta > 1$ by the Higgs mass effects (See (25)). Any other choice of the mixing angle α leads less enhancement. Although we here adopt Model II of the Yukawa couplings in actual calculation in the 2HDM, it is clear that there is no difference between Model I and II for the enhancement of this process because of the above analytic discussion. We use the Fortran FF package for the evaluation of integral functions [18].

To begin with, we compare the $\tan\beta$ dependence of the total cross section in the 2HDM and the MSSM at $\sqrt{s} = 500$ GeV and $m_{H^\pm} = 200$ GeV (Fig 3). The parameters for the

2HDM is taken as $m_{H^0} = 210$ GeV, $m_{h^0} = 100$ GeV and $M = 0$. For the small $\tan\beta$ region, the cross sections are enhanced by the top-quark mass effects both in the 2HDM and the MSSM ². This enhancement is bounded at $\tan\beta \sim 0.2$ (~ 2) in the 2HDM (in the MSSM) by the requirement of validity of perturbation (the requirement of Yukawa unification at GUT scale). Similar property of the top mass effects is observed in the cross section of $e^+e^- \rightarrow A^0V$ ($V = \gamma, Z^0$) [20]. On the other hand, for the large $\tan\beta$ region, the MSSM cross section decreases rapidly, while the Higgs non-decoupling mass effects enlarge the 2HDM cross section. However, we notice that larger $\tan\beta$ ($\gtrsim 8.3$) is excluded for m_{H^0} and $M = 0$ in this case by the condition (28). Fig 4(a) and (b) is the \sqrt{s} dependence of the total cross section at $m_{H^\pm} = 200$ and 260 GeV in the 2HDM for each $\tan\beta$.

The enhancement of the cross section essentially depends on the size of the $H^\pm tb$ and $H^\pm H^\mp H^0$ coupling constants. By taking these couplings as large as possible under the requirement of validity of perturbation (28) and also under the experimental ρ parameter constraints we have mentioned above, we obtain the best enhancement of the cross section in the non-SUSY 2HDM for each m_{H^\pm} . In Fig 5 we show such general bound of the cross section as a function of $\tan\beta$ at $\sqrt{s} = 500$ GeV for $m_{H^\pm} = 160, 200, 240, 280, 320$ and 360, in which all the other free parameters are chosen to obtain maximal enhancement under all the constraints. The peak in the intermediate $\tan\beta$ region is the point where the largest non-decoupling Higgs mass effect with $M = 0$ appears. By the constraint (28), larger values of $\tan\beta$ are allowed only by introducing nonzero soft-breaking mass M . The nonzero M , however, induces the less enhancement because the non-decoupling property of the Higgs sector is reduced by a non-zero M .

Finally we comment on the detectability of the signal events for the case of $m_{H^\pm} > m_t + m_b$. The H^\pm then decays into a tb pair and the signal process is $e^+e^- \rightarrow H^\pm W^\mp \rightarrow t\bar{b}W^- +$

² Our result for the MSSM cross section is somewhat different from that in ref [5]; our result gives the smaller cross section than the other one. The test by using the equivalence theorem [19] agrees with our results.

$\bar{t}bW^+$. The main background process may be $e^+e^- \rightarrow t\bar{t} \rightarrow \bar{b}W^- + \bar{t}bW^+$. The cross section of $e^+e^- \rightarrow t\bar{t}$ amounts to about 0.57 pb for $\sqrt{s} = 500$ GeV; the signal/background ratio is at most around 1 %. It may be, however, expected that the signal can be comfortably seen if the signal cross section is 10fb, by attaining a good background reduction [21] by the following strategy: 1) cut around reconstructed bW masses which can come from bW decay at 175GeV, 2) find a peak in reconstructed m_{H^\pm} and 3) confirm the presence of H^\pm according to the method in Ref. [22]. For the case with a much smaller the signal cross section such as a few 0.1fb, details of the background analysis are needed to see the detectability.

6 Conclusion

We have discussed the H^\pm production process via $e^+e^- \rightarrow H^\pm W^\mp$ in the non-SUSY 2HDM as well as the MSSM. The possible enhancement of the cross section has been explored by the non-decoupling effects of the quarks and the Higgs bosons. In the MSSM, only the top-quark effects contribute to enhancement of the cross section. The maximal enhancement occurs at $\tan\beta \sim 1 - 2$, the lower bound of $\tan\beta$, and it amounts to around a few 0.1 fb for $m_{H^\pm} = 200$ GeV. The cross section decreases for larger $\tan\beta$. In the non-SUSY 2HDM, the larger enhancement is possible by the top-quark mass effects because smaller $\tan\beta$ regime is allowed than in the MSSM, which can be as large as 10 fb for $m_{H^\pm} = 200$ GeV. In addition to these top-quark mass effects, the Higgs mass effects can contribute to the cross section by about 0.1 fb for the intermediate regime of $\tan\beta$, where the top-quark mass effects are small. By the requirement of the validity of perturbation theory, such enhancement due to the Higgs-boson masses is reduced for larger $\tan\beta$. The maximal enhancement in the 2HDM (~ 10 fb at $\tan\beta \sim 0.2 - 0.3$) may be possible to be observed. However, to know the detectability of a few 0.1 fb of the cross section, details of the background analysis are needed.

Acknowledgments

The author would like to thank Wolfgang Hollik for useful discussion, Kosuke Odagiri for valuable discussion on the method of the background reduction, and Yasuhiro Okada for useful information about $\tan\beta$. This work was supported, in part, by Alexander von Humboldt Foundation.

A The MSSM Higgs sector

The supersymmetry imposes the constraint among parameters in the 2HDM. If we set the parameters by the following relation

$$\mu_1^2 = \frac{1}{8}(g^2 + g'^2)v^2 \cos 2\beta - \tan \beta \mu_3^2, \quad (29)$$

$$\mu_2^2 = -\frac{1}{8}(g^2 + g'^2)v^2 \cos 2\beta - \cot \beta \mu_3^2, \quad (30)$$

$$\lambda_1 = \lambda_2 = \frac{1}{8}(g^2 + g'^2), \quad (31)$$

$$\lambda_3 = \frac{1}{4}(g^2 - g'^2), \quad (32)$$

$$\lambda_4 = \lambda_5 = -\frac{1}{2}g^2, \quad (33)$$

the potential (1) becomes the MSSM Higgs potential [17], where $g'^2 = s_W^2 g^2$. These MSSM constraints lead the following tree-level relations among the mass parameters and the mixing angles;

$$m_{A^0}^2 = m_{H^\pm}^2 - m_W^2, \quad (34)$$

$$m_{h,H}^2 = \frac{1}{2} \left\{ m_{A^0}^2 + m_Z^2 \mp \sqrt{(m_{A^0}^2 + m_Z^2)^2 - 4m_{A^0}^2 m_Z^2 \cos^2 2\beta} \right\}, \quad (35)$$

$$M^2 = m_{A^0}^2, \quad (36)$$

$$\sin 2\alpha = -\sin 2\beta \frac{m_{A^0}^2 + m_Z^2}{m_{H^0}^2 - m_{h^0}^2}, \quad (37)$$

$$\cos 2\alpha = -\cos 2\beta \frac{m_{A^0}^2 - m_Z^2}{m_{H^0}^2 - m_{h^0}^2}. \quad (38)$$

By using Eqs (35) - (38), for example, the expression of λ_1 in the non-SUSY 2HDM seen in (2) reproduces Eq. (31)

$$\begin{aligned} \lambda_1 &= \frac{1}{2v^2 \cos^2 \beta} \left\{ \cos^2 \alpha m_{H^0}^2 + \sin^2 \alpha m_{h^0}^2 - \sin^2 \beta M^2 \right\} \\ &= \frac{1}{2v^2 \cos^2 \beta} \left\{ \frac{1}{2} \left(1 - \cos 2\beta \frac{m_{A^0}^2 - m_Z^2}{m_{H^0}^2 - m_{h^0}^2} \right) m_{H^0}^2 + \frac{1}{2} \left(1 + \cos 2\beta \frac{m_{A^0}^2 - m_Z^2}{m_{H^0}^2 - m_{h^0}^2} \right) m_{h^0}^2 - \sin^2 \beta m_{A^0}^2 \right\} \\ &= \frac{m_Z^2}{2v^2} = \frac{1}{8}(g^2 + g'^2). \end{aligned} \quad (39)$$

The enhancement as $\tan\beta$ with fixing α in λ_1 , which we have seen in the 2HDM, disappear in the MSSM, and $\tan\beta$ is thus bounded only from the constraints on the Yukawa interaction.

B Analytic results

In the analytic formulas here, we use the integral functions introduced by Passarino and Vertman [23]. The notation about the tensor coefficients here is based on Ref. [19]. We here write $A(m_f)$ as $A[f]$, $B_{ij}(p_H^2; m_{f_1}, m_{f_2})$ as $B_{ij}[f_1, f_2]$, $C_{ij}(p_H^2, p_W^2, p_V^2; m_{f_1}, m_{f_2}, m_{f_3})$ as $C_{ij}[f_1, f_2, f_3]$, where f_i are the fields with mass m_{f_i} . For the quark diagrams, we define notation $C_{ij}(tbb) = C_{ij}(p_H^2, p_W^2, p_V^2; m_t, m_b, m_b)$ and $C_{ij}(ttb) = C_{ij}(p_H^2, p_W^2, p_V^2; m_t, m_t, m_b)$. We calculate one-loop contributions by 't Hooft-Feynman gauge. Also the functions $J(\alpha, \beta)$, $K(\alpha, \beta)$ and $L(\alpha, \beta)$ defined in Eqs. (24) - (26) are written here as $J_{\alpha\beta}$, $K_{\alpha\beta}$ and $L_{\alpha\beta}$, respectively. The momentum squared of the H^\pm is set on mass shell here, $p_H^2 = m_{H^\pm}^2$.

B.1 Form factors of the $H^\pm W^\mp V^0$ ($V^0 = Z^0, \gamma$) Vertices

We write each contribution to the $H^\pm W^\mp V^0$ form factors X^{HWV} , ($X = F, G$ and H) as $X^{HWV} = X^{HWV(a)} + X^{HWV(b)} + X^{HWV(c)}$ corresponding to Fig 6(a), (b) and (c). $X^{HWV(a)}$ is the contribution of triangle-type diagrams (Fig 6(a)), $X^{HWV(b)}$ represents contributions from the two-point function correction shown in Fig 6(b), and $X^{HWV(c)}$ is tadpole contribution as well as some two-point function corrections written only by the A function (Fig 6(c)).

B.1.1 The $H^+ W^- Z^0$ vertex

The contribution of triangle-type diagrams to F^{HWZ} is calculated as

$$F^{HWZ(a)}(p_H, p_W, p_Z) = \frac{2}{16\pi^2 v^2 c_W}$$

$$\begin{aligned}
& \times \left[- \left\{ K_{\alpha\beta}(m_{H^0}^2 - M^2) + J_{\alpha\beta}(-m_{H^0}^2 + 2m_{H^\pm}^2) \right\} \left\{ C_{24}[H^\pm A^0 H^0] - c_{2W}C_{24}[H^0 H^\pm H^\pm] \right\} \right. \\
& - \left\{ L_{\alpha\beta}(m_{h^0}^2 - M^2) - J_{\alpha\beta}(-m_{h^0}^2 + 2m_{H^\pm}^2) \right\} \left\{ C_{24}[H^\pm A^0 h^0] - c_{2W}C_{24}[h^0 H^\pm H^\pm] \right\} \\
& + J_{\alpha\beta} \left\{ (m_{H^\pm}^2 - m_{H^0}^2)C_{24} \left([w^\pm z^0 H^0] - c_{2W}[H^0 w^\pm w^\pm] \right) - (m_{H^\pm}^2 - m_{h^0}^2)C_{24} \left([w^\pm z^0 h^0] - c_{2W}[h^0 w^\pm w^\pm] \right) \right. \\
& - (m_{H^\pm}^2 - m_{A^0}^2)C_{24} \left([w^\pm H^0 A^0] - [w^\pm h^0 A^0] \right) - m_W^2 C_{24} \left([W^\pm H^0 A^0] - [W^\pm h^0 A^0] \right) \\
& - \frac{c_{2W}}{c_W} m_W^2 C_{24} \left([H^\pm H^0 Z^0] - [H^\pm h^0 Z^0] \right) - m_W^2 \left(4(p_W^2 + p_W \cdot p_Z)C_0 + 2(2p_W + p_Z) \cdot (p_W C_{11} + p_Z C_{12}) \right. \\
& + p_W \cdot p_Z C_{23} + (D-1)C_{24} \left([W^\pm Z^0 H^0] - [W^\pm Z^0 h^0] \right) + c_W^2 m_W^2 \left((p_Z^2 - p_W^2)C_0 - 2p_Z \cdot (p_W C_{11} + p_Z C_{12}) \right. \\
& + p_W \cdot p_Z C_{23} + (D-1)C_{24} \left([H^0 W^\pm W^\pm] - [h^0 W^\pm W^\pm] \right) \\
& - m_Z^2(m_{H^\pm}^2 - m_{H^0}^2)s_W^2 C_0[w^\pm Z^0 H^0] + m_Z^2(m_{H^\pm}^2 - m_{h^0}^2)s_W^2 C_0[w^\pm Z^0 h^0] \\
& - m_W^2(m_{H^\pm}^2 - m_{H^0}^2)s_W^2 C_0[H^0 W^\pm w^\pm] + m_W^2(m_{H^\pm}^2 - m_{h^0}^2)s_W^2 C_0[h^0 W^\pm w^\pm] \\
& \left. + m_W^2 s_W^2 \left(C_{24}[H^0 w^\pm W^\pm] - C_{24}[h^0 w^\pm W^\pm] \right) \right\} + \frac{4N_c}{16\pi^2 v^2 c_W} \left[m_b^2 \tan \beta (-s_W^2 Q_b) \right. \\
& \times \left\{ p_W \cdot (p_W + p_Z)C_{11} + p_Z \cdot (p_W + p_Z)C_{12} + p_W^2 C_{21} + p_Z^2 C_{22} + 2p_W \cdot p_Z C_{23} + DC_{24} \right\} (tbb) \\
& - m_b^2 \tan \beta (T_b - s_W^2 Q_b) \left\{ p_W^2 C_{11} + p_Z \cdot p_Z C_{12} + p_W^2 C_{21} + p_Z^2 C_{22} + 2p_W \cdot p_Z C_{23} + (D-2)C_{24} \right\} (tbb) \\
& - m_t^2 \cot \beta (T_b - s_W^2 Q_b) \left\{ (p_W^2 + p_W \cdot p_Z)C_0 + (2p_W^2 + p_W \cdot p_Z)C_{11} + (p_Z^2 + 2p_W \cdot p_Z)C_{12} \right. \\
& + p_W^2 C_{21} + p_Z^2 C_{22} + 2p_W \cdot p_Z C_{23} + (D-2)C_{24} \left. \right\} (tbb) + m_t^2 \cot \beta (-s_W^2 Q_b) m_b^2 C_0 (tbb) + m_t^2 \cot \beta (-s_W^2 Q_t) \\
& \times \left\{ p_Z \cdot (p_W + p_Z)C_{11} + p_W \cdot (p_W + p_Z)C_{12} + p_Z^2 C_{21} + p_W^2 C_{22} + 2p_W \cdot p_Z C_{23} + DC_{24} \right\} (ttb) \\
& - m_b^2 \tan \beta (T_t - s_W^2 Q_t) \left\{ p_Z^2 C_{11} + p_Z \cdot p_Z C_{12} + p_Z^2 C_{21} + p_W^2 C_{22} + 2p_W \cdot p_Z C_{23} + (D-2)C_{24} \right\} (ttb) \\
& - m_t^2 \cot \beta (T_t - s_W^2 Q_t) \left\{ (p_Z^2 + p_W \cdot p_Z)C_0 + (2p_Z^2 + p_W \cdot p_Z)C_{11} + (p_W^2 + 2p_W \cdot p_Z)C_{12} \right. \\
& \left. + p_Z^2 C_{21} + p_W^2 C_{22} + 2p_W \cdot p_Z C_{23} + 2C_{24} \right\} (ttb) + m_b^2 \tan \beta (-s_W^2 Q_t) m_t^2 C_0 (ttb) \left. \right]. \tag{40}
\end{aligned}$$

The contribution of the diagrams which can be expressed in terms of the B_i functions is given by

$$\begin{aligned}
F^{HWZ(b)}(p_H, p_W, p_Z) &= \frac{2}{16\pi^2 v^2 c_W} \left[\frac{1}{2} \left\{ K_{\alpha\beta}(m_{H^0}^2 - M^2) + J_{\alpha\beta}(-m_{H^0}^2 + 2m_{H^\pm}^2) \right\} \right. \\
& \times \left\{ s_W^2 B_0[H^0 H^\pm]_C + \frac{p_Z^2 - p_W^2}{m_{H^\pm}^2 - m_W^2} c_W^2 (B_0 + 2B_1)[H^0 H^\pm]_B + \frac{m_{H^0}^2 - m_{H^\pm}^2}{m_{H^\pm}^2 - m_W^2} s_W^2 B_0[H^0 H^\pm]_E \right\} \\
& + \frac{1}{2} \left\{ L_{\alpha\beta}(m_{h^0}^2 - M^2) - J_{\alpha\beta}(-m_{h^0}^2 + 2m_{H^\pm}^2) \right\} \left\{ s_W^2 B_0[h^0 H^\pm]_C \right. \\
& \left. + \frac{p_Z^2 - p_W^2}{m_{H^\pm}^2 - m_W^2} c_W^2 (B_0 + 2B_1)[h^0 H^\pm]_B + \frac{m_{h^0}^2 - m_{H^\pm}^2}{m_{H^\pm}^2 - m_W^2} s_W^2 B_0[h^0 H^\pm]_E \right\} \left. \right]
\end{aligned}$$

$$\begin{aligned}
& + \frac{1}{2} J_{\alpha\beta} \left\{ -(m_{H^\pm}^2 - m_{H^0}^2) s_W^2 B_0 [H^0 w^\pm]_C + \frac{1}{2} (m_{H^\pm}^2 - m_{h^0}^2) s_W^2 B_0 [h^0 w^\pm]_C \right. \\
& + m_W^2 s_W^2 \left(B_0(p_W^2; W^\pm H^0)_D - B_0(p_W^2; W^\pm h^0)_D \right) + m_Z^2 s_W^2 B_0 \left(B_0(p_Z^2; Z^0 H^0)_D - B_0(p_Z^2; Z^0 h^0)_D \right) \\
& - \frac{1}{2} \frac{m_W^2}{m_{H^\pm}^2 - m_W^2} s_W^2 \left\{ m_{H^\pm}^2 (B_0 - 2B_1 + B_{21}) + DB_{22} \right\} \left([H^0 W^\pm]_E - [h^0 W^\pm]_E \right) \\
& + \frac{1}{2} m_{H^0}^2 \frac{m_{H^0}^2 - m_{H^\pm}^2}{m_{H^\pm}^2 - m_W^2} s_W^2 B_0 [H^0 w^\pm]_E - \frac{1}{2} m_{h^0}^2 \frac{m_{h^0}^2 - m_{H^\pm}^2}{m_{H^\pm}^2 - m_W^2} s_W^2 B_0 [h^0 w^\pm]_E \\
& + m_W^2 \frac{p_Z^2 - p_W^2}{m_{H^\pm}^2 - m_W^2} c_W^2 (B_0 - B_1) \left([H^0 W^\pm]_B - [h^0 W^\pm]_B \right) \\
& + \frac{m_{H^0}^2 - m_{H^\pm}^2}{m_{H^\pm}^2 - m_W^2} (p_Z^2 - p_W^2) c_W^2 (B_0 + 2B_1) [H^0 w^\pm]_B - \frac{m_{h^0}^2 - m_{H^\pm}^2}{m_{H^\pm}^2 - m_W^2} (p_Z^2 - p_W^2) c_W^2 (B_0 + 2B_1) [h^0 w^\pm]_B \left. \right\} \\
& + \frac{4N_c}{16\pi^2 v^2 c_W} \left[\frac{s_W^2}{m_{H^\pm}^2 - m_W^2} \left\{ (m_b^2 \tan \beta - m_t^2 \cot \beta) \left(m_{H^\pm}^2 (B_1 + B_{21}) + 4B_{22} \right) [tb] \right. \right. \\
& \left. \left. - m_t^2 m_b^2 (\tan \beta - \cot \beta) B_0 [tb] \right\} - \frac{c_W^2}{m_{H^\pm}^2 - m_W^2} (p_Z^2 - p_W^2) \left\{ m_b^2 \tan \beta B_1 + m_t^2 \cot \beta (B_1 + B_0) \right\} [tb] \right] \quad (41)
\end{aligned}$$

The diagrams relevant to the A -function is expressed by

$$F^{HWZ(c)}(p_H, p_W, p_Z) = \frac{1}{16\pi^2 v^2 c_W} \frac{1}{m_{H^\pm}^2 - m_W^2} \left[s_W^2 \left(\tilde{\Pi}_{Hw} - T_1 \right) - c_W^2 (p_Z^2 - m_Z^2) T_2 \right], \quad (42)$$

where

$$T_1 = 16\pi^2 v^2 \{ \sin(\alpha - \beta) T_H + \cos(\alpha - \beta) T_h \}, \quad (43)$$

$$T_2 = 16\pi^2 v^2 \left\{ \frac{1}{m_{H^0}^2} \sin(\alpha - \beta) T_H + \frac{1}{m_{h^0}^2} \cos(\alpha - \beta) T_h \right\}. \quad (44)$$

The tadpole diagrams T_H and T_h , and a part of one-loop contribution to the Hw two-point function which is expressed by A function, $\tilde{\Pi}_{Hw}$, are shown in (54), (55) and (56).

The contribution of the triangle type diagrams to G^{HWZ} and H^{HWZ} are given by

$$\begin{aligned}
G^{HWZ(a)}(p_H, p_W, p_Z) &= \frac{2m_W^2}{16\pi^2 v^2 c_W} \\
&\times \left[- \left\{ K_{\alpha\beta} (m_{H^0}^2 - M^2) + J_{\alpha\beta} (-m_{H^0}^2 + 2m_{H^\pm}^2) \right\} (C_{12} + C_{23}) \left\{ [H^\pm A^0 H^0] - c_{2W} [H^0 H^\pm H^\pm] \right\} \right. \\
&- \left\{ L_{\alpha\beta} (m_{h^0}^2 - M^2) - J_{\alpha\beta} (-m_{h^0}^2 + 2m_{H^\pm}^2) \right\} (C_{12} + C_{23}) \left\{ [H^\pm A^0 h^0] - c_{2W} [h^0 H^\pm H^\pm] \right\} \\
&+ J_{\alpha\beta} \left\{ (m_{H^\pm}^2 - m_{H^0}^2) (C_{12} + C_{23}) [w^\pm z^0 H^0] - (m_{H^\pm}^2 - m_{h^0}^2) (C_{12} + C_{23}) [w^\pm z^0 h^0] \right. \\
&- (m_{H^\pm}^2 - m_{H^0}^2) c_{2W} (C_{12} + C_{23}) [H^0 w^\pm w^\pm] + (m_{H^\pm}^2 - m_{h^0}^2) c_{2W} (C_{12} + C_{23}) [h^0 w^\pm w^\pm] \\
&\left. \left. - (m_{H^\pm}^2 - m_{A^0}^2) (C_{12} + C_{23}) \left\{ [w^\pm H^0 A^0] - [w^\pm h^0 A^0] \right\} \right\} \right]
\end{aligned}$$

$$\begin{aligned}
& -m_W^2 (2C_0 + 2C_{11} + C_{12} + C_{23}) \left([W^\pm H^0 A^0] - [W^\pm h^0 A^0] \right) \\
& - \frac{c_{2W}}{c_W} m_W^2 (-C_{12} + C_{23}) \left([H^\pm H^0 Z^0] - [H^\pm h^0 Z^0] \right) \\
& + m_W^2 (2C_0 - 2C_{11} + 5C_{12} + C_{23}) \left([W^\pm Z^0 H^0] - [W^\pm Z^0 h^0] \right) \\
& + c_W^2 m_W^2 (4C_{11} - 3C_{12} - C_{23}) \left([H^0 W^\pm W^\pm] - [h^0 W^\pm W^\pm] \right) \\
& + m_W^2 s_W^2 (C_{23} - C_{12}) \left([H^0 w^\pm W^\pm] - [h^0 w^\pm W^\pm] \right) \Big\} \\
& + \frac{4N_c m_W^2}{16\pi^2 v^2 c_W} \left[m_b^2 \tan \beta (-s_W^2 Q_b) (C_{12} - C_{11}) (tbb) + m_b^2 \tan \beta (T_b - s_W^2 Q_b) (2C_{23} + C_{12}) (tbb) \right. \\
& + m_t^2 \cot \beta (T_b - s_W^2 Q_b) (C_0 + C_{11} + 2C_{12} + 2C_{23}) (tbb) - m_t^2 \cot \beta (-s_W^2 Q_t) (C_{11} - C_{12}) (tbb) \\
& \left. + m_b^2 \tan \beta (T_t - s_W^2 Q_t) (C_{12} + 2C_{23}) (tbb) + m_t^2 \cot \beta (T_t - s_W^2 Q_t) (C_0 + C_{11} + 2C_{12} + 2C_{23}) (tbb) \right].
\end{aligned} \tag{45}$$

$$\begin{aligned}
H^{HWZ(a)}(p_H, p_W, p_Z) &= \frac{4N_c m_W^2}{16\pi^2 v^2 c_W} \left[m_b^2 \tan \beta (-s_W^2 Q_b) (C_{12} - C_{11}) (tbb) - m_b^2 \tan \beta (T_b - s_W^2 Q_b) C_{12} (tbb) \right. \\
& - m_t^2 \cot \beta (T_b - s_W^2 Q_b) (C_0 + C_{11}) (tbb) + m_t^2 \cot \beta (-s_W^2 Q_t) (C_{11} - C_{12}) (tbb) - m_b^2 \tan \beta (T_t - s_W^2 Q_t) C_{12} (tbb) \\
& \left. - m_t^2 \cot \beta (T_t - s_W^2 Q_t) (C_0 + C_{11}) (tbb) \right]
\end{aligned} \tag{46}$$

There is no contribution from the other diagrams to G^{HWZ} and H^{HWZ} ;

$$G^{HWZ(b)} = G^{HWZ(c)} = H^{HWZ(b,c)} = 0. \tag{47}$$

B.1.2 The $H^+W^-\gamma$ vertex

By doing the similar decomposition to the HWZ vertex, we obtain each contribution for the $H^+W^-\gamma$ vertex.

$$\begin{aligned}
F^{HW\gamma(a)}(p_H, p_W, p_\gamma) &= \frac{4s_W}{16\pi^2 v^2} \times \left[\left\{ K_{\alpha\beta} (m_{H^0}^2 - M^2) + J_{\alpha\beta} (-m_{H^0}^2 + 2m_{H^\pm}^2) \right\} C_{24} [H^0 H^\pm H^\pm] \right. \\
& + \left\{ L_{\alpha\beta} (m_{h^0}^2 - M^2) - J_{\alpha\beta} (-m_{h^0}^2 + 2m_{H^\pm}^2) \right\} C_{24} [h^0 H^\pm H^\pm] \\
& + J_{\alpha\beta} \frac{m_W^2}{2} \left\{ (p_\gamma^2 - p_W^2) C_0 - 2p_\gamma \cdot (p_W C_{11} + p_\gamma C_{12}) + p_W \cdot p_\gamma C_{23} + (D-1) C_{24} \right\} [H^0 W^\pm W^\pm] \\
& - J_{\alpha\beta} \frac{m_W^2}{2} \left\{ (p_\gamma^2 - p_W^2) C_0 - 2p_\gamma \cdot (p_W C_{11} + p_\gamma C_{12}) + p_W \cdot p_\gamma C_{23} + (D-1) C_{24} \right\} [h^0 W^\pm W^\pm] \\
& \left. + J_{\alpha\beta} \frac{m_W^2}{2} (m_{H^\pm}^2 - m_{H^0}^2) C_0 [H^0 W^\pm w^\pm] - J_{\alpha\beta} \frac{m_W^2}{2} (m_{H^\pm}^2 - m_{h^0}^2) C_0 [h^0 W^\pm w^\pm] \right]
\end{aligned}$$

$$\begin{aligned}
& -J_{\alpha\beta} \frac{m_W^2}{2} \left(C_{24}[H^0 w^\pm W^\pm] - C_{24}[h^0 w^\pm W^\pm] \right) \\
& -J_{\alpha\beta}(m_{H^\pm}^2 - m_{H^0}^2)C_{24}[H^0 w^\pm w^\pm] + J(\alpha, \beta)(m_{H^\pm}^2 - m_{h^0}^2)C_{24}[h^0 w^\pm w^\pm] \Big] + \frac{4s_W N_c}{16\pi^2 v^2} \left[m_b^2 \tan \beta Q_b \right. \\
& \times \left\{ p_W \cdot (p_W + p_\gamma) C_{11} + p_\gamma \cdot (p_W + p_\gamma) C_{12} + p_W^2 C_{21} + p_\gamma^2 C_{22} + 2p_W \cdot p_\gamma C_{23} + 4C_{24} \right\} (tbb) \\
& -m_b^2 \tan \beta Q_b \left\{ p_W^2 C_{11} + p_W \cdot p_\gamma C_{12} + p_W^2 C_{21} + p_\gamma^2 C_{22} + 2p_W \cdot p_\gamma C_{23} + 2C_{24} \right\} (tbb) \\
& -m_t^2 \cot \beta Q_b \left\{ (p_W^2 + p_W \cdot p_\gamma) C_0 + (2p_W^2 + p_W \cdot p_\gamma) C_{11} + (p_\gamma^2 + 2p_W \cdot p_\gamma) C_{12} \right. \\
& \quad \left. + p_W^2 C_{21} + p_\gamma^2 C_{22} + 2p_W \cdot p_\gamma C_{23} + 2C_{24} \right\} (tbb) + m_t^2 m_b^2 \cot \beta Q_b C_0 (tbb) \\
& +m_t^2 \cot \beta Q_t \left\{ p_\gamma \cdot (p_W + p_\gamma) C_{11} + p_W \cdot (p_W + p_\gamma) C_{12} + p_\gamma^2 C_{21} + p_W^2 C_{22} + 2p_W \cdot p_\gamma C_{23} + 4C_{24} \right\} (tbb) \\
& -m_b^2 \tan \beta Q_t \left\{ p_\gamma^2 C_{11} + p_g \cdot p_Z C_{12} + p_\gamma^2 C_{21} + p_W^2 C_{22} + 2p_W \cdot p_\gamma C_{23} + 2C_{24} \right\} (tbb) \\
& -m_t^2 \cot \beta Q_t \left\{ (p_\gamma^2 + p_W \cdot p_\gamma) C_0 + (2p_\gamma^2 + p_W \cdot p_\gamma) C_{11} + (p_W^2 + 2p_W \cdot p_\gamma) C_{12} \right. \\
& \quad \left. + p_\gamma^2 C_{21} + p_W^2 C_{22} + 2p_W \cdot p_\gamma C_{23} + 2C_{24} \right\} (tbb) + m_b^2 m_t^2 \tan \beta Q_t C_0 (tbb) \Big]. \tag{48}
\end{aligned}$$

$$\begin{aligned}
F^{HW\gamma(b)}(p_H, p_W, p_\gamma) &= \frac{4 \sin \theta_W}{16\pi^2 v^2} \times \left[-\frac{1}{4} \left\{ K_{\alpha\beta}(m_{H^0}^2 - M^2) + J_{\alpha\beta}(-m_{H^0}^2 + 2m_{H^\pm}^2) \right\} \left\{ B_0[H^0 H^\pm]_C \right. \right. \\
& + \frac{m_{H^0}^2 - m_{H^\pm}^2}{m_{H^\pm}^2 - m_W^2} B_0[H^0 H^\pm]_E - \frac{p_\gamma^2 - p_W^2}{m_{H^\pm}^2 - m_W^2} (B_0 + 2B_1)[H^0 H^\pm]_B \Big\} \\
& - \frac{1}{4} \left\{ L_{\alpha\beta}(m_{h^0}^2 - M^2) - J_{\alpha\beta}(-m_{h^0}^2 + 2m_{H^\pm}^2) \right\} \left\{ B_0[h^0 H^\pm]_C \right. \\
& + \frac{m_{h^0}^2 - m_{H^\pm}^2}{m_{H^\pm}^2 - m_W^2} B_0[h^0 H^\pm]_E - \frac{p_\gamma^2 - p_W^2}{m_{H^\pm}^2 - m_W^2} (B_0 + 2B_1)[h^0 H^\pm]_B \Big\} \\
& + J_{\alpha\beta} \left\{ \frac{1}{4}(m_{H^\pm}^2 - m_{H^0}^2) B_0[H^0 w^\pm]_C - \frac{1}{4}(m_{H^\pm}^2 - m_{h^0}^2) B_0[h^0 w^\pm]_C \right. \\
& - \frac{m_W^2}{2} \left(B_0(p_W^2; W^\pm H^0)_D - B_0(p_W^2; W^\pm h^0)_D \right) \\
& + \frac{1}{4} \frac{m_W^2}{m_{H^\pm}^2 - m_W^2} \left\{ m_{H^\pm}^2 (B_0 - 2B_1 + B_{21}) + DB_{22} \right\} \left([H^0 W^\pm]_E - [h^0 W^\pm]_E \right) \\
& - \frac{m_{H^0}^2}{4} \frac{m_{H^0}^2 - m_{H^\pm}^2}{m_{H^\pm}^2 - m_W^2} B_0[H^0 w^\pm]_E + \frac{m_{h^0}^2}{4} \frac{m_{h^0}^2 - m_{H^\pm}^2}{m_{H^\pm}^2 - m_W^2} B_0[h^0 w^\pm]_E \\
& + \frac{1}{2} \frac{m_{H^0}^2 - m_{H^\pm}^2}{m_{H^\pm}^2 - m_W^2} (p_\gamma^2 - p_W^2) (B_0 + 2B_1) [H^0 w^\pm]_B - \frac{1}{2} \frac{m_{H^0}^2 - m_{H^\pm}^2}{m_{H^\pm}^2 - m_W^2} (p_\gamma^2 - p_W^2) (B_0 + 2B_1) [h^0 w^\pm]_B \\
& + \frac{m_W^2}{2} \frac{p_\gamma^2 - p_W^2}{m_{H^\pm}^2 - m_W^2} (B_0 - B_1) [H^0 W^\pm]_B - \frac{m_W^2}{2} \frac{p_\gamma^2 - p_W^2}{m_{H^\pm}^2 - m_W^2} (B_0 - B_1) [h^0 W^\pm]_B \Big\} \Big] \\
& + \frac{4s_W}{16\pi^2 v^2} \left[-\frac{p_\gamma^2 - p_W^2}{m_{H^\pm}^2 - m_W^2} \left\{ m_b^2 \tan \beta B_1 + m_t^2 \cot \beta (B_1 + B_0) \right\} [tb] \right.
\end{aligned}$$

$$-\frac{1}{m_{H^\pm}^2 - m_W^2} \left\{ (m_b^2 \tan \beta - m_t^2 \cot \beta) (m_{H^\pm}^2 (B_1 + B_{21}) + 4B_{22}) + m_t^2 m_b^2 (\tan \beta - \cot \beta) B_0 \right\} [tb] \Bigg]. \quad (49)$$

$$F^{HW\gamma(c)}(p_H, p_W, p_\gamma) = -\frac{sw}{16\pi^2 v^2} \frac{1}{m_{H^\pm}^2 - m_W^2} \left\{ \tilde{\Pi}_{Hw} - T_1 + p_\gamma^2 T_2 \right\}. \quad (50)$$

where T_1 and T_2 and $\tilde{\Pi}_{Hw}$ are defined in (43), (44) and (56).

$$\begin{aligned} G^{HW\gamma(a)}(p_H, p_W, p_\gamma) &= \frac{4m_W^2 sw}{16\pi^2 v^2} \\ &\times \left[\left\{ K_{\alpha\beta}(m_{H^0}^2 - M^2) + J_{\alpha\beta}(-m_{H^0}^2 + 2m_{H^\pm}^2) \right\} (C_{12} + C_{23}) [H^0 H^\pm H^\pm] \right. \\ &+ \left\{ L_{\alpha\beta}(m_{h^0}^2 - M^2) - J_{\alpha\beta}(-m_{h^0}^2 + 2m_{H^\pm}^2) \right\} (C_{12} + C_{23}) [h^0 H^\pm H^\pm] \\ &+ J_{\alpha\beta} \left\{ \frac{m_W^2}{2} (4C_{11} - 3C_{12} - C_{23}) [H^0 W^\pm W^\pm] - \frac{m_W^2}{2} (4C_{11} - 3C_{12} - C_{23}) [h^0 W^\pm W^\pm] \right. \\ &+ \frac{m_W^2}{2} \left((C_{12} - C_{23}) [H^0 w^\pm W^\pm] - (C_{12} - C_{23}) [h^0 w^\pm W^\pm] \right) \\ &\left. \left. - (m_{H^\pm}^2 - m_{H^0}^2) (C_{12} + C_{23}) [H^0 w^\pm w^\pm] + (m_{H^\pm}^2 - m_{h^0}^2) (C_{12} + C_{23}) [h^0 w^\pm w^\pm] \right\} \right] \\ &+ \frac{4m_W^2 sw N_c}{16\pi^2 v^2} \left[m_b^2 \tan \beta Q_b (C_{12} - C_{11}) (tbb) + m_b^2 \tan \beta Q_b (2C_{23} + C_{12}) (tbb) \right. \\ &+ m_t^2 \cot \beta Q_b (C_0 + C_{11} + 2C_{12} + 2C_{13}) (tbb) + m_t^2 \cot \beta Q_t (C_{12} - C_{11}) (tbb) \\ &\left. + m_b^2 \tan \beta Q_t (2C_{23} + C_{12}) (tbb) + m_t^2 \cot \beta Q_t (C_0 + C_{11} + 2C_{12} + 2C_{23}) (tbb) \right]. \quad (51) \end{aligned}$$

$$\begin{aligned} H^{HW\gamma(a)}(p_H, p_W, p_\gamma) &= \frac{4m_W^2 sw N_c}{16\pi^2 v^2} \left[m_b^2 \tan \beta Q_b (C_{12} - C_{11}) (tbb) - m_b^2 \tan \beta Q_b C_{12} (tbb) \right. \\ &- m_t^2 \cot \beta Q_b (C_0 + C_{11}) (tbb) + m_t^2 \cot \beta Q_t (C_{11} - C_{12}) (tbb) - m_b^2 \tan \beta Q_t C_{12} (tbb) \\ &\left. - m_t^2 \cot \beta Q_t (C_0 + C_{11}) (tbb) \right]. \quad (52) \end{aligned}$$

and

$$G^{HW\gamma(b,c)} = H^{HW\gamma(b,c)} = 0. \quad (53)$$

The tadpole graphs $i T_H$ and $i T_h$ are calculated as

$$T_H = \frac{1}{16\pi^2 v} \left[m_{H^0}^2 \cos(\alpha - \beta) \left(A[w^\pm] + \frac{1}{2} A[z^0] \right) \right]$$

$$\begin{aligned}
& + \left\{ \left(\frac{\cos \alpha \sin^2 \beta}{\cos \beta} - \frac{\sin \alpha \cos^2 \beta}{\sin \beta} \right) m_{H^0}^2 + 2 \cos(\alpha - \beta) m_{H^\pm}^2 + \frac{\sin(\alpha + \beta)}{\sin \beta \cos \beta} M^2 \right\} A[H^\pm] \\
& + \left\{ \left(\frac{\cos \alpha \sin^2 \beta}{\cos \beta} - \frac{\sin \alpha \cos^2 \beta}{\sin \beta} \right) m_{H^0}^2 + 2 \cos(\alpha - \beta) m_{A^0}^2 + \frac{\sin(\alpha + \beta)}{\sin \beta \cos \beta} M^2 \right\} \frac{1}{2} A[A^0] \\
& + \frac{3}{2} \left\{ \left(\frac{\cos^3 \alpha}{\cos \beta} + \frac{\sin^3 \alpha}{\sin \beta} \right) m_{H^0}^2 - \frac{\cos 2\beta}{\cos \beta \sin \beta} \sin(\alpha - \beta) M^2 \right\} A[H^0] \\
& + \left\{ \frac{1}{2} (m_{H^0}^2 + 2m_{h^0}^2) \frac{\sin 2\alpha}{\sin 2\beta} - \frac{M^2}{4 \cos \beta \sin \beta} (-3 \sin 2\alpha + \sin 2\beta) \right\} \cos(\alpha - \beta) A[h^0] \\
& + 8 \cos(\alpha - \beta) \left(m_W^2 A[W^\pm] + \frac{1}{2} m_Z^2 A[Z^0] \right) - 4N_c \left(\frac{\cos \alpha}{\cos \beta} A[b] + \frac{\sin \alpha}{\sin \beta} A[t] \right) \Big], \tag{54}
\end{aligned}$$

$$\begin{aligned}
T_h &= \frac{1}{16\pi^2 v} \left[-m_{h^0}^2 \sin(\alpha - \beta) \left(A[w^\pm] + \frac{1}{2} A[z^0] \right) \right. \\
& + \left\{ \left(\frac{\sin \alpha \sin^2 \beta}{\cos \beta} - \frac{\cos \alpha \cos^2 \beta}{\sin \beta} \right) m_{h^0}^2 - 2 \sin(\alpha - \beta) m_{H^\pm}^2 + \frac{\cos(\alpha + \beta)}{\sin \beta \cos \beta} M^2 \right\} A[H^\pm] \\
& + \left\{ \left(\frac{\sin \alpha \sin^2 \beta}{\cos \beta} - \frac{\cos \alpha \cos^2 \beta}{\sin \beta} \right) m_{h^0}^2 - 2 \sin(\alpha - \beta) m_{A^0}^2 + \frac{\cos(\alpha + \beta)}{\sin \beta \cos \beta} M^2 \right\} \frac{1}{2} A[A^0] \\
& - \frac{3}{2} \left\{ \left(\frac{\sin^3 \alpha}{\cos \beta} - \frac{\cos^3 \alpha}{\sin \beta} \right) m_{h^0}^2 + \frac{\cos 2\beta}{\cos \beta \sin \beta} \cos(\alpha - \beta) M^2 \right\} A[h^0] \\
& + \frac{1}{2} \left\{ (2m_{H^0}^2 + m_{h^0}^2) \frac{\sin 2\alpha}{\sin 2\beta} - \frac{M^2}{4 \cos \beta \sin \beta} (3 \sin 2\alpha + \sin 2\beta) \right\} \sin(\alpha - \beta) A[H^0] \\
& \left. - 8 \sin(\alpha - \beta) \left(m_W^2 A[W^\pm] + \frac{1}{2} m_Z^2 A[Z^0] \right) - 4N_c \left(\frac{\sin \alpha}{\cos \beta} A[b] + \frac{\cos \alpha}{\sin \beta} A[t] \right) \right]. \tag{55}
\end{aligned}$$

Finally, $\Pi_{Hw} (= \tilde{\Pi}_{Hw} / (16\pi^2 v^2))$ is given by

$$\begin{aligned}
\Pi_{Hw} &= \frac{1}{16\pi^2 v^2} \left[2(m_{H^0}^2 - m_{h^0}^2) J_{\alpha\beta} \left(A[W^\pm] + \frac{1}{4} A[Z^0] \right) \right. \\
& + 2 \left\{ K_{\alpha\beta} - J_{\alpha\beta} - \frac{\sin(\alpha + \beta)}{\sin \beta \cos \beta} M^2 \right\} m_{H^0}^2 A[H^\pm] + 2 \left\{ L_{\alpha\beta} + J_{\alpha\beta} - \frac{\cos(\alpha + \beta)}{\sin \beta \cos \beta} M^2 \right\} m_{h^0}^2 A[H^\pm] \\
& + \frac{1}{4} \left\{ \sin 2\beta \left(\frac{\sin^2 \alpha}{\sin^2 \beta} - \frac{\cos^2 \alpha}{\cos^2 \beta} \right) - \sin 2(\alpha - \beta) \right\} m_{H^0}^2 A[A^0] \\
& + \frac{1}{4} \left\{ \sin 2\beta \left(\frac{\cos^2 \alpha}{\sin^2 \beta} - \frac{\sin^2 \alpha}{\cos^2 \beta} \right) + \sin 2(\alpha - \beta) \right\} m_{h^0}^2 A[A^0] - \cot 2\beta M^2 A[A^0] \\
& + J_{\alpha\beta} m_{H^\pm}^2 (A[h^0] - A[H^0]) + \frac{1}{4} \sin 2\beta \left(\frac{\sin^4 \alpha}{\sin^2 \beta} - \frac{\cos^4 \alpha}{\cos^2 \beta} + \frac{\sin 2\alpha \cos 2\alpha}{\sin 2\beta} \right) m_{H^0}^2 A[H^0] \\
& + \frac{1}{4} \sin 2\beta \left(\frac{\sin^2 \alpha \cos^2 \alpha}{\sin^2 \beta} - \frac{\sin^2 \alpha \cos^2 \alpha}{\cos^2 \beta} - \frac{\sin 2\alpha \cos 2\alpha}{\sin 2\beta} \right) m_{h^0}^2 A[H^0] \\
& \left. - \frac{M^2}{2} \frac{\cos 2\beta}{\cos \beta \sin \beta} (\sin^2(\alpha - \beta) A[H^0] + \cos^2(\alpha - \beta) A[h^0]) \right]
\end{aligned}$$

$$\begin{aligned}
& + \frac{1}{4} \sin 2\beta \left(\frac{\sin^2 \alpha \cos^2 \alpha}{\sin^2 \beta} - \frac{\cos^2 \alpha \sin^2 \alpha}{\cos^2 \beta} - \frac{\sin 2\alpha}{\sin 2\beta} \cos 2\alpha \right) m_{H^0}^2 A[h^0] \\
& + \frac{1}{4} \sin 2\beta \left(\frac{\cos^4 \alpha}{\sin^2 \alpha} - \frac{\sin^4 \alpha}{\cos^2 \beta} + \frac{\sin 2\alpha \cos 2\alpha}{\sin 2\beta} \right) m_{h^0}^2 A[h^0] \Big].
\end{aligned} \tag{56}$$

B.2 The t channel contribution

The contribution of the t -channel diagram (Fig 1(b)) is only from the W^+H^- mixing.

When we write the $W^\mu H$ two-point function as

$$i\Pi_{WH}^\mu(p) = ip^\mu \Pi_{WH}(p^2), \tag{57}$$

the contribution to the form factor is expressed as

$$F_{1,\tau}^t = \delta_{i,1} \delta_{\tau,-1} \frac{g^2}{2} \frac{1}{m_{H^\pm}^2 - m_W^2} \Pi_{WH}(m_{H^\pm}). \tag{58}$$

The the $W^\mu H$ two-point function is calculated as

$$\begin{aligned}
\Pi_{WH}(m_{H^\pm}^2) &= \frac{m_W}{16\pi^2 v^2} \left[2m_W^2 J_{\alpha\beta} \left\{ (B_0 - B_1)[H^0 W^\pm] - (B_0 - B_1)[h^0 W^\pm] \right\} \right. \\
&+ \left\{ K_{\alpha\beta} m_{H^0}^2 + J_{\alpha\beta} (-m_{H^0}^2 + 2m_{H^\pm}^2) \right\} (2B_1 + B_0) [H^0 H^\pm] \\
&+ \left\{ L_{\alpha\beta} m_{h^0}^2 - J_{\alpha\beta} (-m_{h^0}^2 + 2m_{H^\pm}^2) \right\} (2B_1 + B_0) [h^0 H^\pm] \\
&+ (m_{H^0}^2 - m_{H^\pm}^2) J_{\alpha\beta} (2B_1 + B_0) [H^0 w^\pm] - (m_{h^0}^2 - m_{H^\pm}^2) J_{\alpha\beta} (2B_1 + B_0) [h^0 w^\pm] \\
&\left. - 4N_c \left\{ m_b^2 \tan \beta B_1 + m_t^2 \cot \beta (B_1 + B_0) \right\} [tb] - T_2 \right],
\end{aligned} \tag{59}$$

where the tadpole contribution T_2 is given in (44).

B.3 The box-diagram

The contribution from the box diagrams (Fig 1(c)) is parametrised as

$$F_{i,\tau}^{\text{box}} = -\frac{1}{16\pi^2} \frac{g^4}{4} m_W J_{\alpha\beta} \left\{ f_i^{\text{box}}[\nu, W, H^0, W] - f_i^{\text{box}}[\nu, W, h^0, W] \right\} \delta_{\tau,-1}. \tag{60}$$

The functions f_i^{box} are calculated as

$$\begin{aligned}
f_1^{\text{box}}[\nu, W, S, W] = & \left\{ 2(t - m_{H^\pm}^2)D_{11} + 2m_{H^\pm}^2D_{12} + (s - m_{H^\pm}^2 - m_W^2)D_{13} \right. \\
& + m_{H^\pm}^2D_{22} + m_W^2D_{23} + (t - m_{H^\pm}^2)D_{24} + (-s - t + m_{H^\pm}^2)D_{25} \\
& \left. + (s - m_{H^\pm}^2 - m_W^2)D_{26} + 4D_{27} \right\} [\nu, W, S, W], \tag{61}
\end{aligned}$$

$$f_2^{\text{box}}[\nu, W, S, W] = m_W^2 D_{13}[\nu, W, S, W], \tag{62}$$

$$f_3^{\text{box}}[\nu, W, S, W] = m_W^2 \left(\frac{1}{2} D_{11} + D_{13} \right) [\nu, W, S, W], \tag{63}$$

where

$$D_{ij}[\nu, W, S, W] = D_{ij}(k^2, p_H^2, p_W^2, \bar{k}^2; 0, m_W, m_S, m_W), \quad (S = h^0, H^0). \tag{64}$$

References

- [1] *Physics and Technology of the Next Linear Collider: a Report submitted to Snowmass 1996*, BNL 52-502, FNAL-PUB-96/112, LBNL-PUB-5425, SLAC Report 485, UCRL-ID-124160; *JLC-1*, KEK Report 92-16 (1992).
- [2] S. Kanemura, Phys. Rev. D, in press, (hep-ph/9710237).
- [3] A. Méndez and A. Pomarol, Nucl. Phys. **B349**, 369 (1991); M. Capdequi Peyranère, H.E. Haber and P. Irulegui, Phys. Rev. D **44**, 191 (1991).
- [4] A. Arhrib, M. Capdequi Peyranère and G. Moutaka, Phys. Lett. **B 341**, 313 (1995); J. Guasch, W. Hollik and A. Kraft, talk at the Vth eorkshop in the 2nd ECFA/DESY Study on Physics and Detectors For a Linear Electron-Positron Collider, Obernai (France) 16-19th Oct. 1999 (hep-ph/9911452).
- [5] S.H. Zhu, (hep-ph/9901221).
- [6] T. Appelquist and J. Carrazone, Phys. Rev. D **11**, 2856 (1975).
- [7] V. Barger, M.S. Berger and P. Ohmann, Phys.Rev. D **47**, 1093 (1993); M. Carena, M. Olechowski, S. Pokorski and C.E.M. Wagner, Nucl. Phys. **B426**, 269 (1994).
- [8] DELPHI: LEPC talks, Presentations on Nov 9 1999,
(http://delphiwww.cern.ch/offline/physics_links/lepc.html)
- [9] Y. Grossman, Nucl. Phys. **B426**, 355 (1994).
- [10] P. Ciafaloni and D. Esprin, Phys. Rev. D **56**, 1752 (1997).
- [11] S. Kanemura, T. Kasai and Y. Okada, Phys. Lett. **B**, in press (hep-ph/9903289).
- [12] S. Kanemura and H-A. Tohyama, Phys. Rev. D **57**, 2949 (1998).
- [13] S. Kanemura, T. Kubota and E. Takasugi, Phys. Lett. **B313**, 155 (1993).

- [14] P.H. Chankowski, M. Krawczyk and J. Zochowski, CERN-TH/99-133, IFT-98/20 (hep-ph/9905436); A.K. Grant, Phys. Rev. D **51**, 207 (1995).
- [15] CLEO Collaboration, CLEO CONF 98-17, ICHEP98 1011.
- [16] F. Borzumati, C. Greub, Phys. Rev. D **58**, 074004 (1998); *ibid* D **59**, 057501 (1999).
- [17] J.F. Gunion, H.E. Haber, G. Kane and S. Dawson, *The Higgs Hunter's Guide*, (Addison-Wesley, New York, 1990).
- [18] G.J. van Oldenborgh and J.A.M. Vermaseren, Comput. Phys. Commun. **66**, 1 (1991), Z. Phys. **C46**, 425 (1990).
- [19] S. Alam, K. Hagiwara, S. Kanemura, R. Szalapski and Y. Umeda, Nucl. Phys. **B541**, 50 (1999).
- [20] A.G. Akeroyd, A. Arhrib and M. Capequi Peyran  re, KEK Preprint 99/53, LPM/99/31, UFR-HEP/99/17, (hep-ph/9907542 v2 1Aug 1999).
- [21] K. Odagiri, private communication.
- [22] K. Odagiri, Phys. Lett. **B452**, 327 (1999).
- [23] G. Passarino and M. Veltman, Nucl. Phys. **B160**, 151 (1979).

TABLE CAPTION

Table 1: The list of the kinematical coefficient $K_{i,\tau}(\lambda)$.

FIGURE CAPTIONS

Fig 1: The diagrams for $e^+e^- \rightarrow H^-W^+$. The circles in (a), and (b) represent all one-loop diagrams relevant to the HWV vertices ($V = \gamma, Z^0$) and the HW mixing. The arrows on the H^\pm bosons and the W boson lines indicate the flow of negative electric charge.

Fig 2: The HWV vertices ($V = \gamma, Z^0$). The arrows on the H^\pm boson and the W boson lines indicate the flow of negative electric charge.

Fig 3: The $\tan\beta$ dependence of the total cross section of $e^+e^- \rightarrow H^-W^+$ at $\sqrt{s} = 500$ GeV for $m_{H^\pm} = 200$ GeV in the 2HDM (solid lines) and the MSSM (dashed line). For the 2HDM, three lines correspond to $m_{A^0} = 300, 600$ and 1200 GeV. The other parameters are chosen as $\alpha = \beta - \pi/2$, $m_{h^0} = 80$ GeV and $m_{H^0} = 210$ GeV.

Fig 4: The \sqrt{s} dependence of the total cross section of $e^+e^- \rightarrow H^-W^+$ at $m_{H^\pm} = 200$ GeV in the non-SUSY 2HDM for $\tan\beta = 0.3, 0.5, 1, 2, 4$ (Solid lines) and $8, 16$ (Dotted lines). The other parameters are chosen as $\alpha = \beta - \pi/2$, $m_{h^0} = 80$ GeV and $m_{H^0} = m_{H^\pm} + 10$ GeV.

Fig 5: The possible enhancement of the total cross section of $e^+e^- \rightarrow H^-W^+$ in the non-SUSY 2HDM under the experimental ρ -parameter constraint and under the requirement of validity of the perturbation theory (27). The cross sections are given as a function of $\tan\beta$ for each value of m_{H^\pm} .

Fig 6(a) The first group of the Feynman diagrams ('t Hooft-Feynman gauge) of the HWV vertices ($V = \gamma, Z^0$), which corresponds to $X^{HWV(a)}$ ($X = F, G$ and H) in

Appendix B.

Fig 6(b) The second group of the Feynman diagrams ('t Hooft-Feynman gauge) of the HWV vertices ($V = \gamma, Z^0$), which corresponds to $X^{HWV(b)}$ ($X = F, G$ an H) in Appendix B.

Fig 6(c) The third group of the Feynman diagrams ('t Hooft-Feynman gauge) of the HWV vertices ($V = \gamma, Z^0$), which corresponds to $X^{HWV(c)}$ ($X = F, G$ an H) in Appendix B.

	$K_{1,\tau}(\lambda)$	$K_{2,\tau}(\lambda)$	$K_{3,\tau}(\lambda)$
$\lambda = 0$	$-\frac{1}{2m_W}(s - m_{H^\pm}^2 + m_W^2) \sin \Theta$	$\frac{1}{2} \frac{s^2}{m_W^3} \beta_{HW}^2 \sin \Theta$	0
$\lambda = \pm$	$\sqrt{\frac{s}{2}}(\mp \cos \Theta + \tau)$	0	$-\frac{s}{m_W^2} \sqrt{\frac{s}{2}} \beta_{HW} (\cos \Theta \mp \tau)$

Table 1

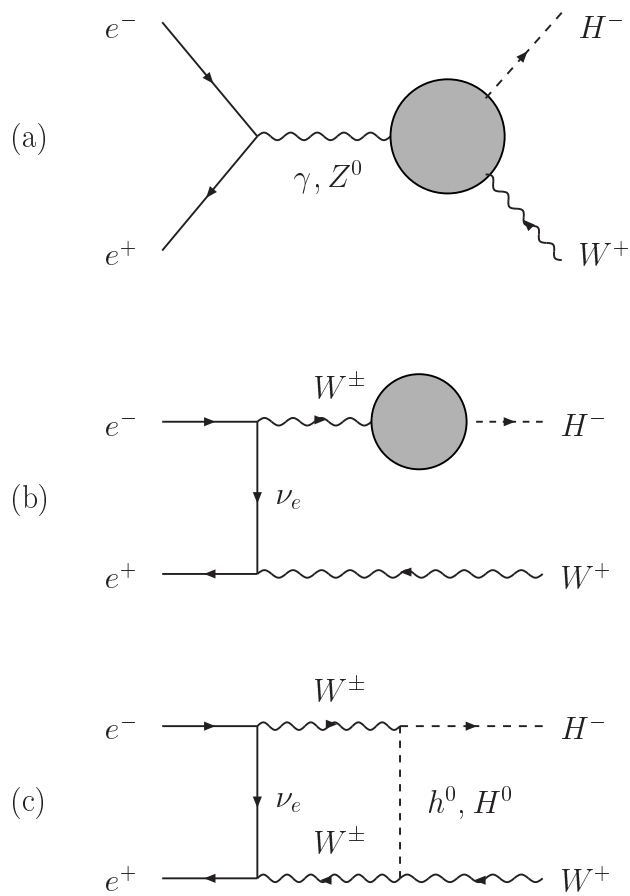


Figure 1

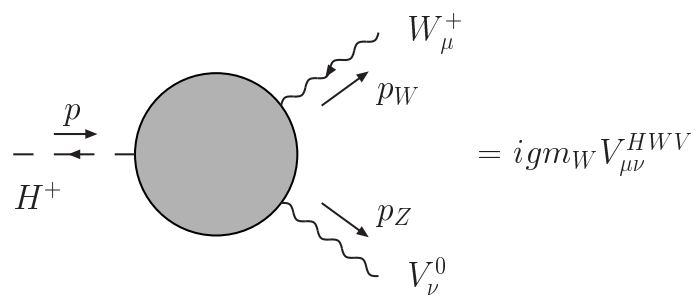


Figure 2

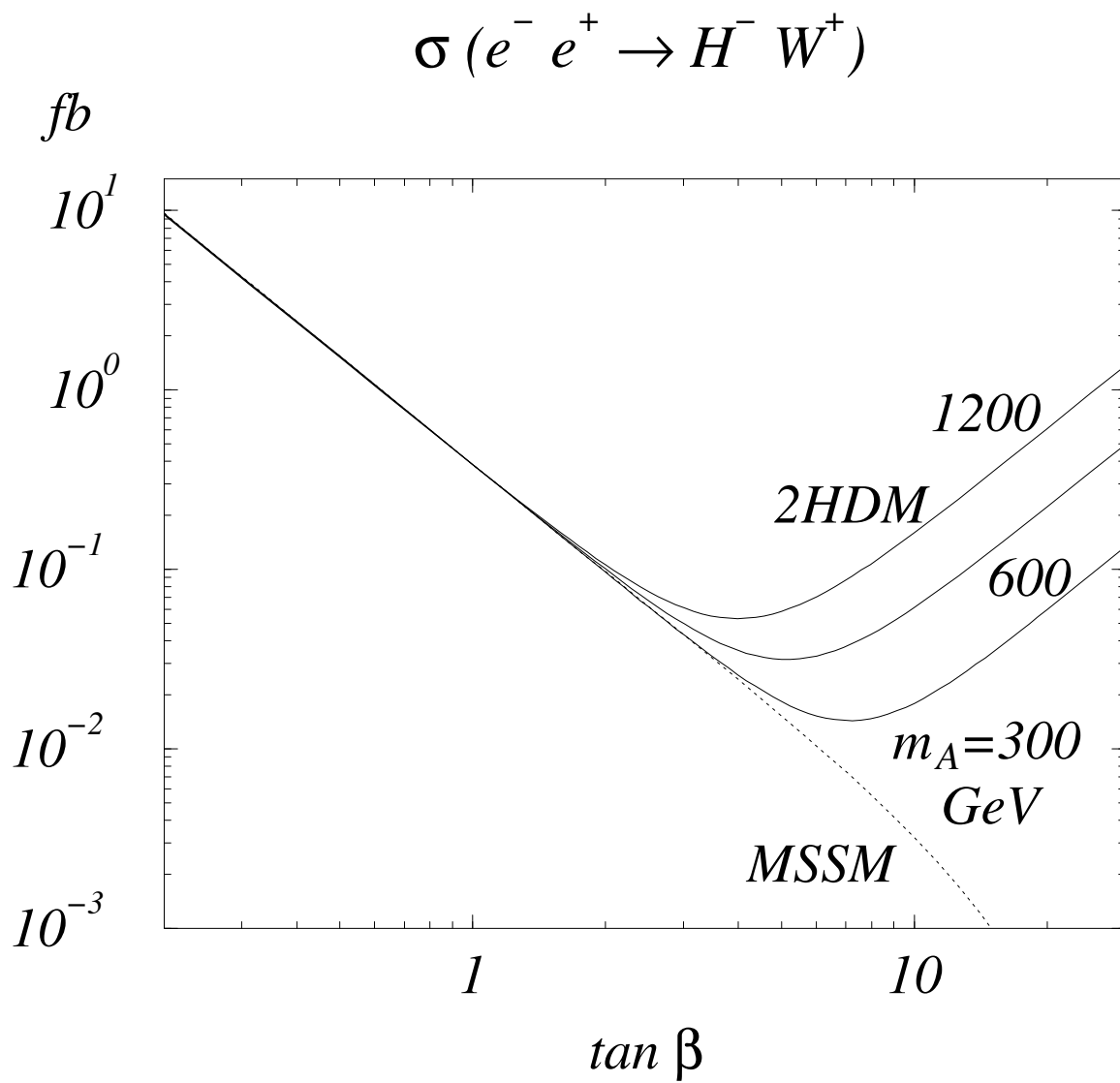


Figure 3

$$\sigma(e^-e^+ \rightarrow H^-W^+)$$

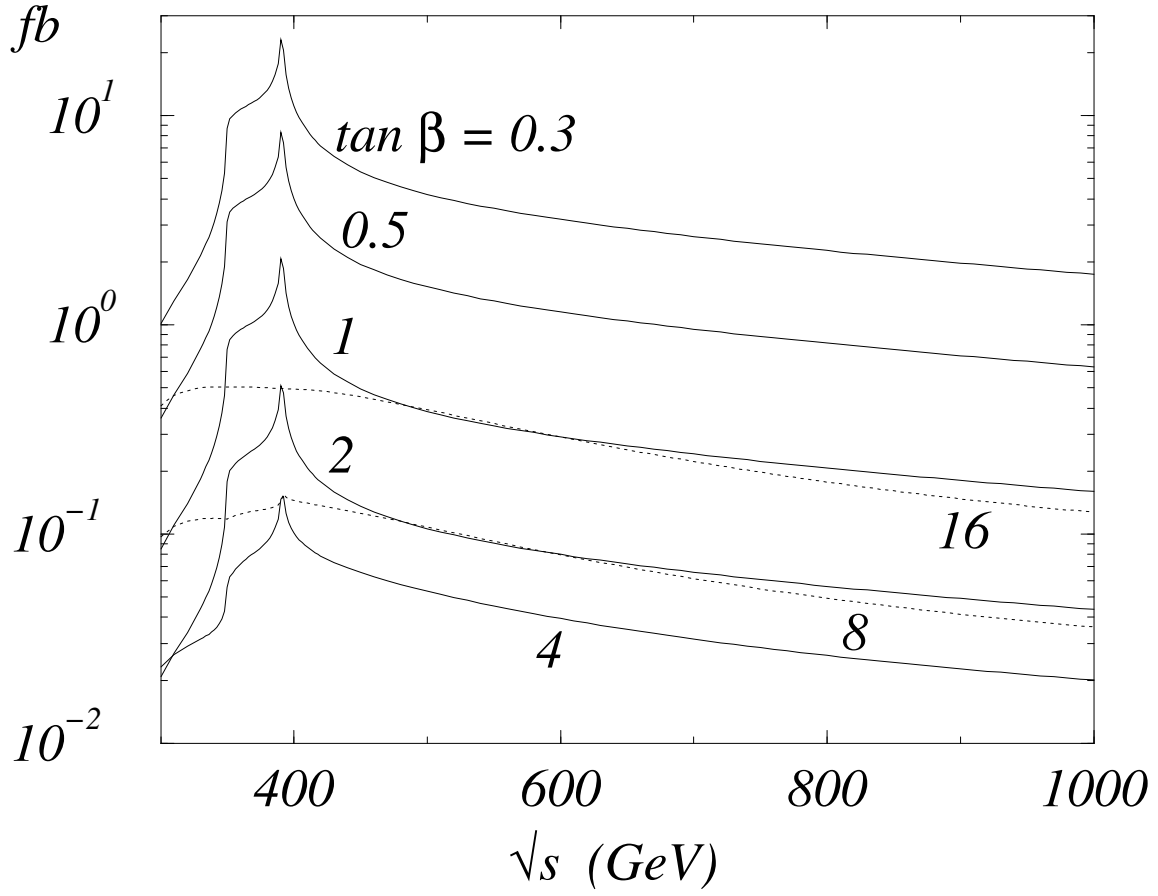


Figure 4

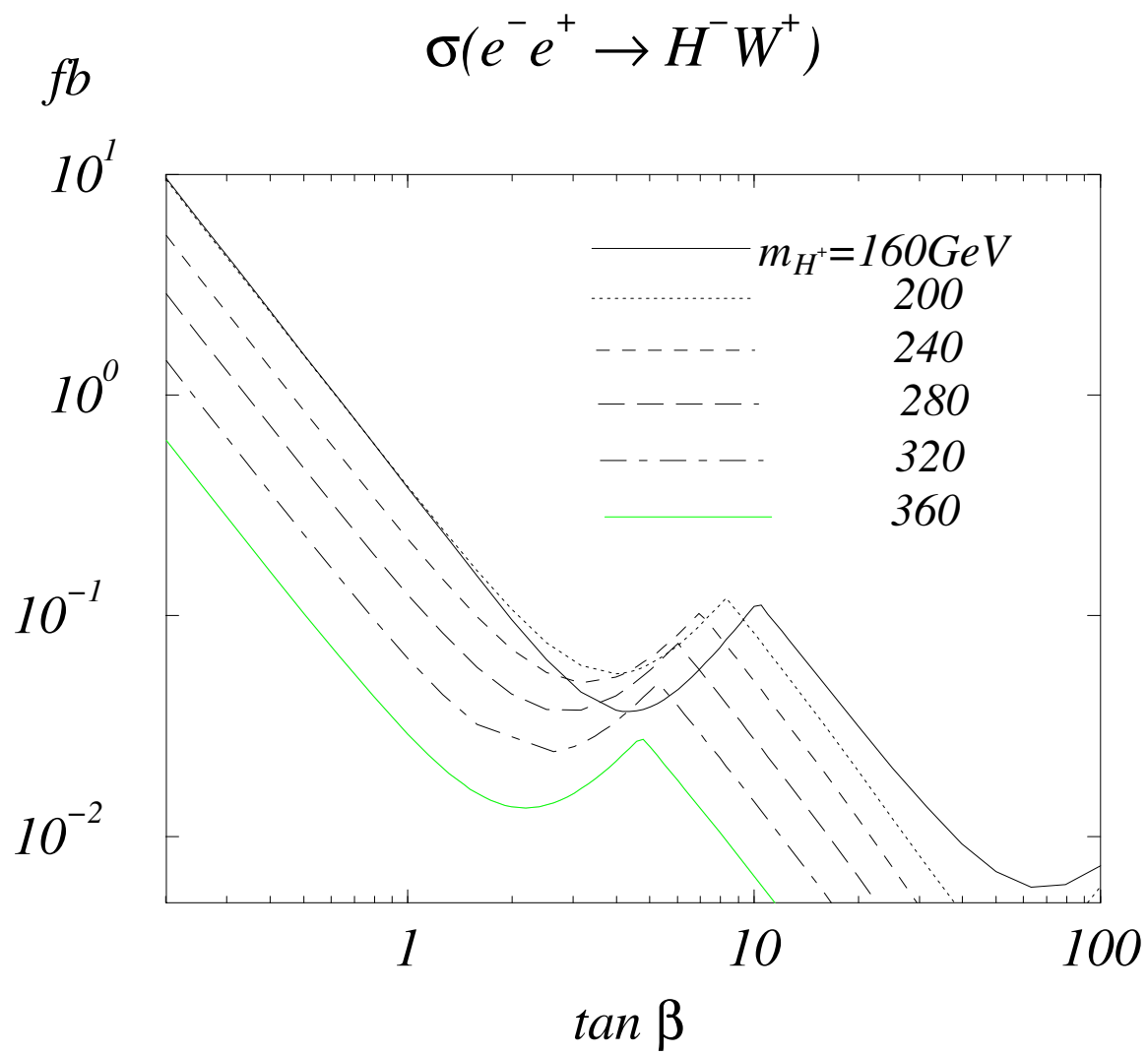


Figure 5

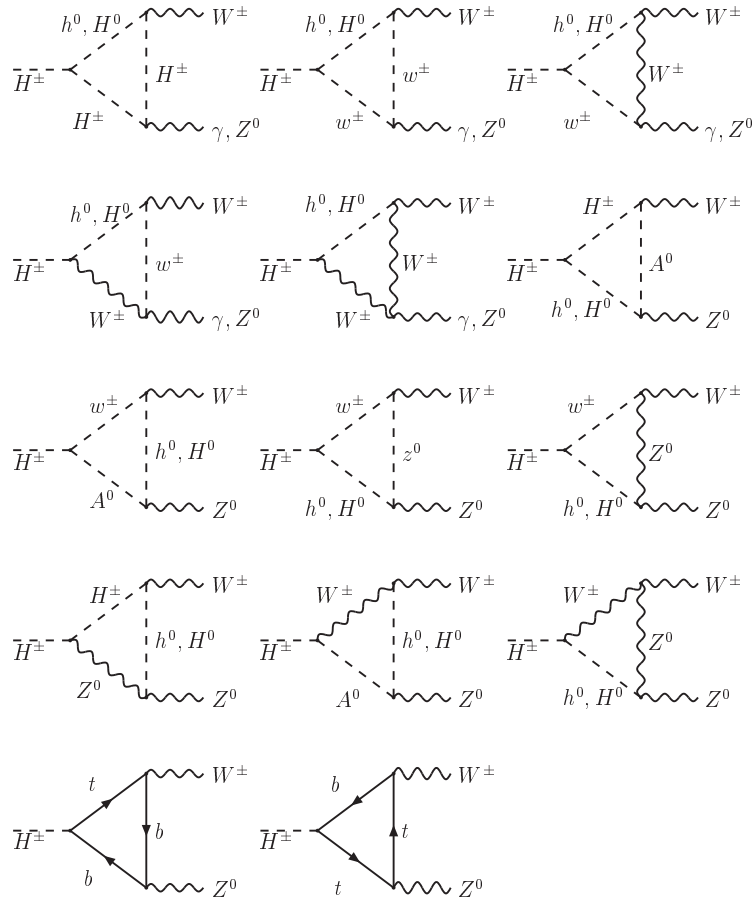


Figure 6(a)

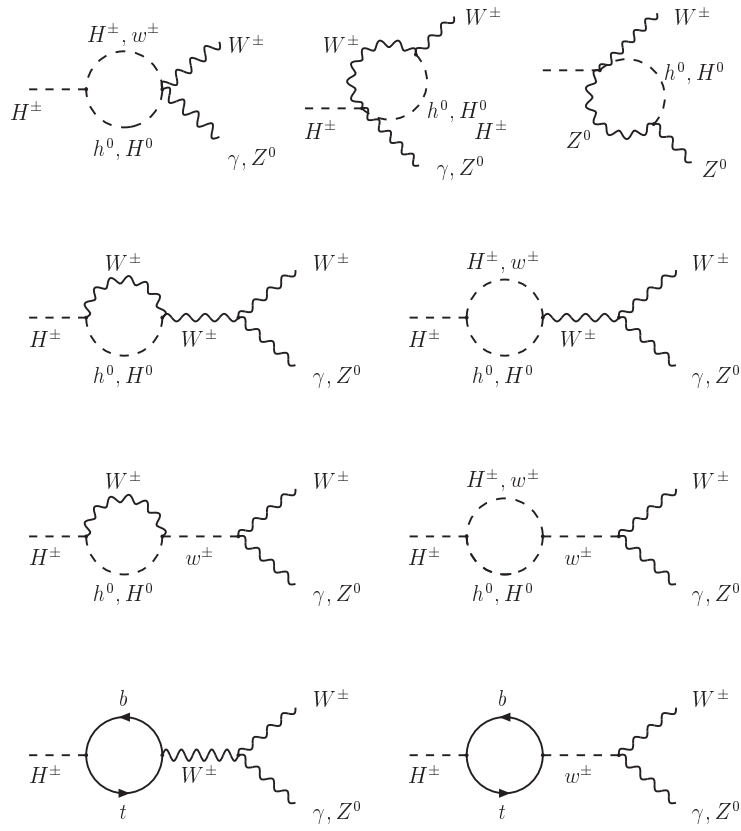


Figure 6(b)

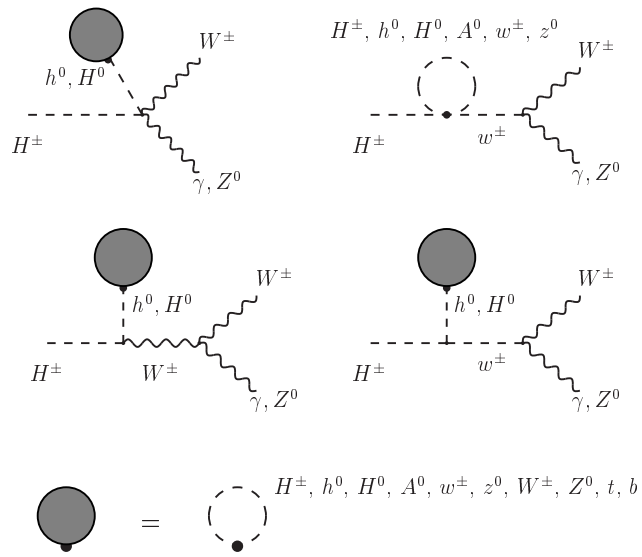


Figure 6(c)